TERRESTRIAL BIOSPHERE CARBON STORAGE UNDER ALTERNATIVE CLIMATE PROJECTIONS

SIBYLL SCHAPHOFF[1], WOLFGANG LUCHT[1], DIETER GERTEN[1], STEPHEN SITCH[1], WOLFGANG CRAMER[1] and I. COLIN PRENTICE[2]

[1]*Potsdam Institute for Climate Impact Research, P.O. Box 601203, D-14412 Potsdam, Germany*
E-mail: sibylls@pik-potsdam.de
[2]*QUEST, Department of Earth Sciences, University of Bristol, Wills Memorial Building, Bristol BS8 1RJ, UK*

Abstract. This study investigates commonalities and differences in projected land biosphere carbon storage among climate change projections derived from one emission scenario by five different general circulation models (GCMs). Carbon storage is studied using a global biogeochemical process model of vegetation and soil that includes dynamic treatment of changes in vegetation composition, a recently enhanced version of the Lund-Potsdam-Jena Dynamic Global Vegetation Model (LPJ-DGVM). Uncertainty in future terrestrial carbon storage due to differences in the climate projections is large. Changes by the end of the century range from −106 to +201 PgC, thus, even the sign of the response whether source or sink, is uncertain. Three out of five climate projections produce a land carbon source by the year 2100, one is approximately neutral and one a sink. A regional breakdown shows some robust qualitative features. Large areas of the boreal forest are shown as a future CO_2 source, while a sink appears in the arctic. The sign of the response in tropical and sub-tropical ecosystems differs among models, due to the large variations in simulated precipitation patterns. The largest uncertainty is in the response of tropical rainforests of South America and Central Africa.

1. Introduction

The land biosphere plays a substantial role in the global carbon cycle. In the 1990s, an average of 6.4 PgC/yr (billion tons per year) were emitted from fossil fuel burning. Net carbon uptake by the land is estimated as 1.0 ± 0.8 PgC/yr (Bopp et al., 2002; Plattner et al., 2002; House et al., 2003). This figure is smaller than the IPCC estimate of 1.4 ± 0.7 PgC/yr based on CO_2 and O_2 measurements (Prentice et al., 2001), as the more recent estimates account for the effects of warming on oceanic stratification and thus on the amount of O_2 stored in the ocean. The net carbon uptake however represents the balance of two terms: the additional carbon emitted due to ongoing land use change (which is currently dominated by tropical deforestation), and carbon taken up by ecosystems through natural processes including the fertilization effect of increasing atmospheric CO_2 (Prentice et al., 2001). The emission due to land use change in the 1990s is thought to be in the range 1.4 to 3.0 PgC/yr (House et al., 2003) implying that terrestrial ecosystems elsewhere are taking up 1.6 to 4.8 PgC/yr and thus significantly reducing the rate of atmospheric CO_2 build-up and the attendant change in climate.

Climatic Change (2006) 74: 97–122
DOI: 10.1007/s10584-005-9002-5

Climate change due to anthropogenic increase of atmospheric greenhouse gas concentrations has an impact upon the carbon balance of the terrestrial biosphere in several ways. CO_2 fertilization and associated improvements in plant water use efficiency lead to increased vegetation growth (Amthor, 1998; DeLucia et al., 1999). Changing climate also affects plant growth through shifts in seasonal cycles, for example due to shifts in precipitation patterns or longer growing seasons (Myneni et al., 1997). Changes in plant growth may in turn lead to biogeographical changes in vegetation distribution and composition. Net uptake of carbon occurs where gains due to increased growth or decreased decomposition outweigh losses, whereas net release of carbon from the biosphere may occur where soil decomposition rates in a warmer climate begin to exceed the productivity of plants, or where changes in vegetation composition lead to a loss of woody biomass (White et al., 2000).

Simulations using coupled land-ocean-atmosphere climate models show a large positive feedback between climate and the carbon cycle, and in particular identify the major role of the terrestrial carbon cycle (Cox et al., 2000; Joos et al., 2001; Friedlingstein et al., 2001; Dufresne et al., 2002). These studies show that the expected effect of continuing warming is to reduce carbon sequestration in the land biosphere, that is, climate warming may be amplified through higher net release of carbon to the atmosphere. Simulations have indicated that the biosphere is likely to turn into a net carbon source by the end of the 21st century (Cox et al., 2000; Joos et al., 2001). The strength of the feedback, however, is still under debate (Jones et al., 2003; Friedlingstein et al., 2003) as models differ in their distribution of carbon uptake between vegetation, soils and ocean due to differences in climate sensitivity of key processes and turnover rates. Cox et al. (2000) project terrestrial carbon cycle feedbacks on the order of -170 PgC (from 2000 to 2100). A previous study of the response of six dynamic vegetation models to one climate scenario suggested that the annual rate of terrestrial carbon storage is likely to continue to increase until the year 2050 and then saturate (Cramer et al., 2001). Some of the models presented in that study showed a subsequent decline in the annual rate of carbon storage, though none strongly enough to produce a strong carbon source by the year 2100. Nonetheless, these simulations underlined the point that one should not assume that continued stimulation of plant growth due to climate change automatically results in long-term increased rates of annual carbon sequestration.

The focus of this study is on commonalities and differences in projected land biosphere carbon storage (potential natural vegetation) among climate change projections derived from one emission scenario by different general circulation models (GCMs). It adds to the study by Cramer et al. (2001) by exploring the response of an enhanced version of one of the biosphere models used in that study to five climate scenarios. We employ a process model of carbon and water plant biogeochemistry, soil dynamics and transient vegetation biogeography, the Lund-Potsdam-Jena Dynamic Global Vegetation Model (LPJ-DGVM) (Sitch et al., 2003).

2. Methods

2.1. THE LPJ DYNAMIC GLOBAL VEGETATION MODEL

The LPJ-DGVM (Sitch et al., 2003) is a process-based model representing key ecosystem processes governing terrestrial biogeochemistry and biogeography. At the core of the model, the Farquhar-Collatz photosynthesis scheme (Farquhar et al., 1980; Collatz et al., 1992) is coupled to a two-layered soil hydrological scheme (Neilson, 1995) that allows realistic simulations of gross primary production (GPP) and plant respiration (Haxeltine and Prentice, 1996b) including effects of drought stress on assimilation and evapotranspiration (Gerten et al., 2004). Subtracting plant respiration from GPP gives the net primary production (NPP). Maintenance respiration is calculated daily based on tissue specific C:N ratios, tissue biomass and phenology (Ryan,1991 and Sprugel et al., 1995) and a modified Arrhenius temperature dependent formulation (Lloyd and Taylor 1994). This assimilated carbon is allocated annually to four pools (leaves, sapwood, heartwood and fine roots) to satisfy a set of allometric and functional relations (Sitch et al., 2003). Leaf and root turnover, as well as plant mortality, redistribute carbon to a litter and to a slow and a fast soil carbon pool. Above-ground litter decomposition depends on air temperature whereas below-ground litter and soil organic matter decomposition are calculated using soil temperature and a modified Arrhenius formulation (Lloyd and Taylor 1994), which implies a realistic decline in apparent Q_{10} values with temperature, and an empirical soil moisture relationship by Foley (1995).

Vegetation functional differences are represented by nine plant functional types (PFTs), which may in principle co-exist at any location, depending on plant competition and a set of environmental constraints. Seven woody and two herbaceous strategies are differentiated by their physiological (C3 or C4 photosynthesis), physiognomic (woody or herbaceous) and phenological (deciduous or evergreen) attributes. Their relative proportion is determined by competition among types with typical ecological strategies for dealing with temperature, water and light stress. Fire disturbance is simulated as a function of a threshold litter load and surface soil moisture (Thonicke et al., 2001). Vegetation structure and composition adjust dynamically to changes in climate so that transient carbon balances can be simulated on various time scales, including effects such as climate-induced tree invasion or dieback, or vegetation changes following shifts in the production-respiration balance.

The LPJ-DGVM has been comprehensively validated for terrestrial carbon and water exchanges and vegetation distribution. The model correctly projects seasonal cycles of atmospheric CO_2 at different latitudes (Sitch et al., 2003), the observed trend in seasonal cycle amplitude of atmospheric carbon dioxide concentrations since the 1960s (McGuire et al., 2001) and interannual variability in its growth rate (Prentice et al., 2000) as well as realistic global patterns of foliage cover and vegetation type (Sitch et al., 2003). The validity of simulated macroscale global fluxes of water (Gerten et al., 2004), of spatial patterns of soil moisture using global

satellite data (Wagner et al., 2003) and of soil moisture seasonality at test sites (Sitch et al., 2003) has been demonstrated. Agreement of modelled with satellite-observed leaf area index anomalies in the circumpolar boreal zone (Lucht et al., 2002) demonstrates consistency of the temperature dependence of modelled NPP while qualitative agreement of modelled land-atmosphere flux with atmospheric inversion results indicates qualitatively correct behaviour of the net carbon balance. Uncertainties in predicting respiration processes are common to all current biosphere models.

The current work is based on an improved version of the LPJ model. Compared to earlier versions (Cramer et al., 2001; Sitch et al., 2003), the treatment of the hydrological cycle has been improved to enhance the realism of water stress effects on vegetation and to take into account leaf interception losses and evaporation fluxes (Gerten et al., 2004). The model experiment intentionally neglects the feedback from terrestrial carbon changes to atmospheric CO_2 and land use effects to carbon cycling in order to isolate the response of the climate and biosphere to a single trajectory of CO_2 concentration. Global NPP in the 1990s is simulated to be 64 PgC/yr with a land sink of 1.8 PgC/yr, which is on the lower limit of estimations of the residual terrestrial sink (1.6 to 4.8 PgC/yr) with CO_2-, O_2- and $^{13}CO_2$-based budgets of terrestrial and ocean carbon uptake (House et al., 2003).

2.2. GENERAL CIRCULATION MODELS AND EMISSION SCENARIO

We applied scenario results from the following five general circulation models to the LPJ-DGVM. All of these participated in the Coupled Model Intercomparison Project (CMIP)/Atmospheric Model Intercomparison Project (AMIP). (1) The Canadian Centre for Climate Modelling and Analysis' CGCM1/MOM1.1 model (Flato et al., 2000), (2) the Hamburg Max Planck Institute for Meteorology's ECHAM4/OPYC3 model (Roeckner et al., 1996), (3) the University of Tokyo Center for Climate System Research's and Japanese National Institute of Environmental Studies' CCSR/NIES model (Emori et al., 1999), (4) the Australian Commonwealth Scientific and Industrial Research Organisation's (CSIRO) Atmospheric Research Mark 2b model (Hirst et al., 1996), (5) and the United Kingdom Meteorological Office Hadley Centre's HadCM3 model (Gordon et al., 2000). Each of these models is a fully coupled atmosphere-ocean model operating at geographical grid resolutions between 2° and 6° degrees and resolving vertical processes on between 10 and 20 layers in both atmosphere and ocean.

The magnitude of climate change projected by a GCM directly depends on the specification of greenhouse gas (and aerosol) forcing. Anthropogenic carbon emissions from fossil fuel burning may take one of many very different courses (Scenario after Nakicenovic and Swart, 2000), but it is probably inevitable that, before the end of the 21st century, the CO_2 concentration in the atmosphere will have at least doubled from pre-industrial levels (IPCC, WG I, 2001). We base our investigations

on climate simulations assuming the IS92a scenario, a business as usual emission scenario with medium assumptions about population increase and economic growth until the year 2100 (Houghton et al., 1992). The scenario is not intended to be economically realistic, it assumes an annual increase of anthropogenic greenhouse gas emissions by 1% from 7.1 PgC/yr in 2000 to 20.4 PgC/yr in 2100 (IPCC WGI, Appendix, 2001). Forcings other than those from greenhouse gases, such as from sulphate aerosols, were not considered. For the direct effects of CO_2 on primary production, data for 1860−1999 are prescribed using a spline fit of Mauna Loa and ice core data. The future period (2000–2100) was created by processing the IS92a emission data with the revised Bern global carbon cycle model taking into account the reference case which includes a mid-range estimate of the terrestrial carbon cycle feedback (Prentice et al., 2001, IPCC WGI, Appendix, 2001). Ambient CO_2 concentration reaches 703 ppmv in 2100.

2.3. PROJECTED CLIMATE CHANGE

Simulated increases in land surface mean annual temperature, measured as the difference between the 1971–2000 and the 2071–2100 global averages, are in a range from +3.7 °C to +6.2 °C (Table I). Increases in annual precipitation over land range between +6.5% and +13.8% (Table I). The relative agreement between results from the different models is less in individual seasons than for the annual mean.

All models simulate pronounced temperature increases over land surfaces in the northern hemisphere, reaching up to 10 °C in high latitudes for the CGCM1 scenario (Figure 1). This model also shows strong warming in central Asia. In the southern hemisphere, models show a temperature increase of up to 3.8 °C, with the CGCM1 scenario showing up to 6.7 °C increase in some regions of Africa. The latter model generally produces the greatest temperature changes among the climate models, while CCSR shows the most pronounced interannual variability. However, broad spatial patterns of increase are similar between models.

In contrast, there are major differences among GCMs in projected changes in precipitation (Figure 1). All models project slight increases in global precipitation, but the regional patterns differ greatly. HadCM3 shows a distinct decrease in Amazonia, and a relatively small increase in precipitation at the high northern latitudes. CSIRO produces the largest increase in precipitation in the northern hemisphere with little change in the southern. ECHAM4, in contrast, shows varying regional patterns of precipitation change in the southern hemisphere. Most striking are two opposing projections in South America, with a large increase in precipitation over northwest and central areas of the continent and a prominent decrease in the northeast and the southwest. For central Africa, ECHAM4, HadCM3 and CCSR project a substantial increase in precipitation with slight decreases elsewhere in Africa, while CGCM1 projects a reduction over the whole continent. For the Indian subcontinent

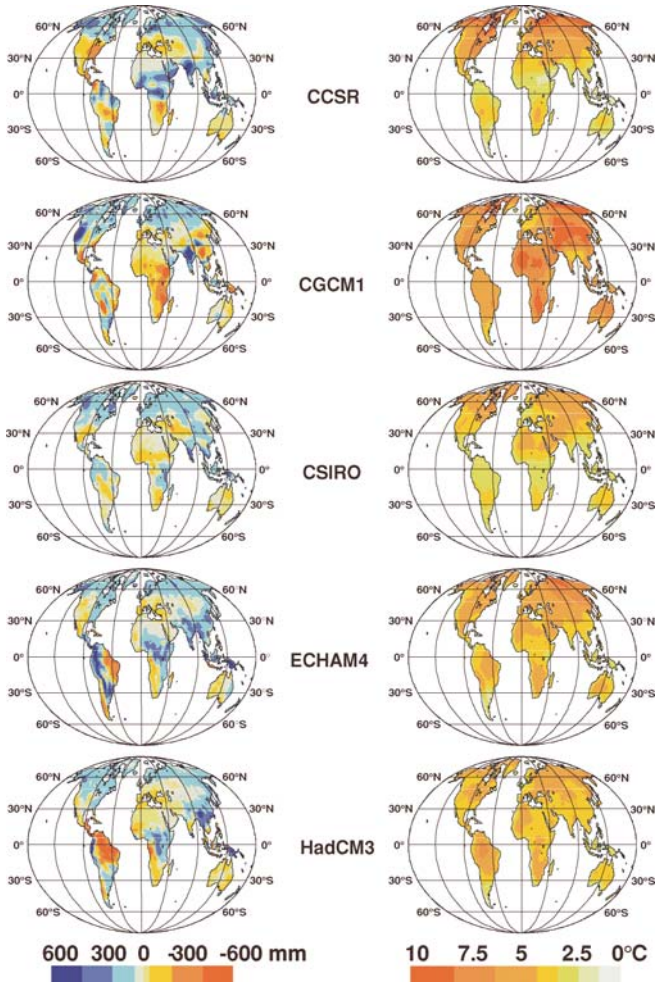

Figure 1. Changes in annual precipitation [mm] (left) and in annual mean surface air temperature [°C] (right), 2071–2100 vs. 1971–2000, as projected by the 5 GCMs.

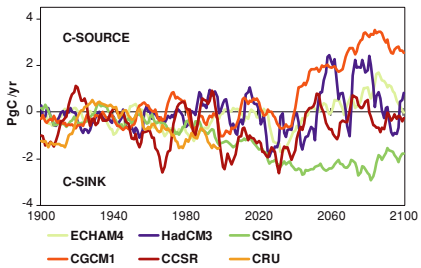

Figure 2. Time series of global land-atmosphere flux [PgC/yr] projected by LPJ under different climate scenarios.

all models project a precipitation increase with the exception of HadCM3, which shows only small precipitation changes. For Europe the model of CSIRO produces the scenario with the least extreme changes, while the other models show distinct precipitation changes with decreases in the South and increases in the North. In the North, their magnitudes are similar between models, but they differ in the South. In East Asia all models project modest to large increases in precipitation except for CGCM1, which projects a reduction.

2.4. FORCING OF THE LPJ-DGVM WITH CLIMATE SCENARIOS

Monthly climate data from each of the five GCM simulations were spatially interpolated to a regular global latitude-longitude grid of 0.5° resolution. Anomalies of the climate data were computed and superimposed onto the 1961–1990 average of observed monthly climate taken from the University of East Anglia's Climatic Research Unit's (CRU) 0.5° global gridded climate data set (New et al., 2000). Annual carbon stocks and fluxes were calculated from the LPJ-DGVM by forcing the model with the resulting monthly temperature, precipitation and radiation data from the GCM simulations, IS92a-based annual ambient CO_2 concentrations, soil texture, and number of monthly rain days (based for the entire future series on the 30-year 1961–1990 mean of the CRU dataset). Soil texture data from the FAO soil data set (FAO, 1991) based on Zobler (1986) were used. The model was run with a 990-year spin-up using the first 30 years of the climate data set used in a particular simulation followed by the entire transient climate scenario; only the period from 1900 to 2100 was evaluated. Additionally, the model was run with the CRU dataset of observed climate from 1900 to 1998 as a baseline simulation. Current and future land use changes were not considered as our focus was on the background response of non-cropland ecosystems to CO_2 and climate.

3. Results

We assess long-term changes (Table I) in the total amount of carbon stored in the land biosphere (the sum of all carbon pools in vegetation, litter and soils) as the difference between 30-year averages at the end of the 20th and 21st centuries (1971–2000 vs. 2071–2100). Annual net fluxes of carbon are expressed as land-atmosphere fluxes, which are the annual differences between NPP, soil respiration and emissions from fires. We follow the IPCC convention that a positive flux represents a flux of CO_2 from the terrestrial biosphere into the atmosphere, i.e. a biosphere source.

3.1. GLOBAL TERRESTRIAL CARBON CYCLE

Present day (1971–2000) simulated NPP based on the climate simulated by the five GCMs ranges between 58 and 64 PgC/yr (Table I). This compares well with the LPJ

TABLE I
Projected changes in carbon pools and annual fluxes, and in climate, presented as average differences between 2071–2100 and 1971–2000

		1971–2000	2071–2100	Δ	Δ (%)
Land-atmosphere flux	LPJ-ECHAM4	−0.5	+0.7	+1.2	
(R_h+fireC-NPP) [PgC/yr]	LPJ-CSIRO	−1.1	−1.8	−0.7	
	LPJ-HadCM3	+0.1	+1.1	+1.0	
LPJ-CRU 1.26	LPJ-CGCM1	−0.5	+2.9	+3.4	
	LPJ-CCSR	−0.6	−0.2	+0.4	
	Average	−0.5	+0.5	+1.0	
NPP	LPJ-ECHAM4	62.6	75.7	13.1	13.0
[PgC/yr]	LPJ-CSIRO	63.7	84.4	20.7	20.7
	LPJ-HadCM3	61.9	74.1	12.2	12.2
LPJ-CRU 63.00	LPJ-CGCM1	61.9	71.8	9.9	9.9
	LPJ-CCSR	58.4	74.2	15.8	15.8
	Average	61.7	76.0	14.3	23.2
Soil respiration	LPJ-ECHAM4	57.4	70.4	13.0	22.6
[PgC/yr]	LPJ-CSIRO	57.7	76.2	18.5	32.2
	LPJ-HadCM3	57.1	69.2	12.1	21.3
LPJ-CRU 57.20	LPJ-CGCM1	56.4	69.1	12.7	22.6
	LPJ-CCSR	53.3	68.2	14.9	27.9
	Average	56.4	70.6	14.2	25.3
Total Carbon	LPJ-ECHAM4	2277	2282	5	0.2
[PgC]	LPJ-CSIRO	2352	2553	201	8.6
	LPJ-HadCM3	2264	2245	−19	−0.8
LPJ-CRU 2333	LPJ-CGCM1	2302	2196	−106	−4.6
	LPJ-CCSR	2082	2162	80	3.8
	Average	2255	2288	33	1.4
Vegetation Carbon	LPJ-ECHAM4	721	772	51	7.1
[PgC]	LPJ-CSIRO	807	958	151	18.7
	LPJ-HadCM3	689	694	5	0.7
LPJ-CRU 779	LPJ-CGCM1	720	712	−8	−1.1
	LPJ-CCSR	577	653	76	13.2
	Average	703	758	55	7.7
Soil Carbon	LPJ-ECHAM4	1556	1510	−46	−2.9
[PgC]	LPJ-CSIRO	1544	1595	51	3.3
	LPJ-HadCM3	1574	1551	−24	−1.5
LPJ-CRU 1554	LPJ-CGCM1	1582	1484	−98	−6.2
	LPJ-CCSR	1505	1509	4	0.2
	Average	1552	1530	−23	−1.5

(*Continued on next page*)

TABLE I
(*Continued*)

		1971–2000	2071–2100	Δ	Δ (%)
Temperature	LPJ-ECHAM4	13.4	17.7	4.3	
[degrees C]	LPJ-CSIRO	13.4	17.1	3.7	
	LPJ-HadCM3	13.4	17.3	3.9	
LPJ-CRU 13.3	LPJ-CGCM1	13.6	19.5	6.2	
	LPJ-CCSR	13.4	17.7	4.4	
	Average	13.4	17.9	4.4	
Precipitation	LPJ-ECHAM4	124241	141355	17114	13.8
[km^3/yr]	LPJ-CSIRO	124158	139358	15200	12.2
	LPJ-HadCM3	123641	131632	7991	6.5
LPJ-CRU 121469	LPJ-CGCM1	122615	133722	11107	9.1
	LPJ-CCSR	123370	134988	11618	9.4
	Average	123605	136211	12606	10.2

baseline of 63 PgC/yr using the actual historical climatology and is similar to other estimates ranging between 45 and 60 PgC/yr (Cramer et al. 1999). Vegetation carbon ranges between 577 and 807 PgC for the present day (baseline 779 PgC), which is in line with literature estimates ranging between 466 and 654 PgC (IPCC, 2001) and 640 PgC (Cao and Woodward, 1998). Estimates of the size of contemporary soil carbon storage range from 1505 to 1582 PgC, similar to estimates of IPCC of 1567 PgC (IPCC, 2001) and a baseline of 1554 PgC. Present-day land-atmosphere flux in the 1990s ranges between a small source of 0.1 PgC/yr to a sink of 1.1 PgC/yr, in the range of estimates of land-atmosphere flux of -1.0 ± 0.8 from House et al. (2003).

Modelled land-atmosphere fluxes from the different climate scenarios diverge from the beginning of the 21st century onward (Figure 2). The magnitude of carbon storage and of interannual fluctuations increases. Some simulations show strong fluctuations between source and sink behaviour during the first half of the century. After 2040 the magnitude of annual terrestrial carbon uptake is reduced in four out of five model runs, and in three of them the terrestrial biosphere becomes a carbon source. The highest land-atmosphere flux achieved is about -2.5 PgC/yr in the LPJ-CSIRO simulation from 2040 and this carbon sink almost stabilises in magnitude thereafter. By 2100 the thirty-year average land-atmosphere flux ranges between -1.8 PgC/yr (LPJ-CSIRO) and $+2.9$ PgC/yr (LPJ-CGCM1), the model average being $+0.5$ PgC/yr (Figure 2, Table I). These results can be explained by considering projected climate changes from the individual GCMs on NPP, stocks and turnover times of carbon in biomass and soil pools.

By 2100, global NPP increases in the model average to 76 PgC/yr, a 23% increase relative to the present day. Increases in NPP range between 16% for

LPJ-CGCM1 and 32% for LPJ-CSIRO. As we assume a constant rate of CO_2 increase for all scenarios, the difference in magnitude of NPP increase between models is necessarily due to the climate changes. CSIRO and CGCM1 respectively are at the lower and upper ranges of projected future temperature (Table I). The modest NPP increases shown in LPJ-CGCM1 are due to these high temperatures and an associated increase in water stress and the adapted vegetation cover.

The size of the vegetation carbon pool is a function of NPP and plant mortality. Despite increases in NPP for all models, two models (LPJ-CGCM1, LPJ-HadCM3), which show the lowest increases in NPP, suggest only minor changes in biomass (less than 10 PgC or 1%) while three models show large increases between 50 (LPJ-ECHAM4) and 150 PgC (LPJ-CSIRO) (Table I), with an average increase over models of 55 PgC. LPJ-CGCM1 and LPJ-HadCM3 show the strongest effects of water stress on NPP and increasing plant mortality, due to large regional reductions in precipitation, in particular in Amazonia in LPJ-HadCM3, and with large global temperature increases in LPJ-CGCM1.

The size of the soil carbon pool is a function of the litter input, and hence indirectly of NPP (since a large portion of NPP is allocated to the leaves and fine roots, which have a fast turnover time, and enters the litter/soil pools after a few years), and the heterotrophic respiration rate, which is a function of temperature and soil moisture. By 2100, the five climate scenarios show changes in the soil carbon pool that range between a decrease of 98 PgC or 6.2% (LPJ-CGCM1) and an increase of 51 PgC or 3.3% (LPJ-CSIRO), on average a small decrease of 23 PgC or 1.5% (Table I). In LPJ-CGCM1 the largest reduction in soil carbon is projected due to the combined effect of high temperatures (Figure 1), which enhances the heterotrophic respiration rate, and a modest increase in litter input via NPP. In contrast, LPJ-CSIRO projects the largest increase in NPP and biomass, maintaining an increased litter input into the soils. This counteracts the relatively modest increase in respiration rate, produced by the smallest increase among models in future global temperatures and moderate precipitation changes.

Total carbon storage in 2071–2100 is estimated to be in the model average as 2288 PgC, which amounts to a small increase of 32 PgC or 1.5% relative to the present day (Table I, Figure 3). By 2100 two model simulations indicate changes of less than 20 PgC (LPJ-HadCM3, LPJ-ECHAM4), while increases of 80 and 201 PgC are projected for LPJ-CCSR and LPJ-CSIRO respectively. LPJ-CGCM1 shows a decrease of 106 PgC, with almost no change in biomass and substantial losses in soil carbon induced by the effects on increasing heterotrophic respiration rates and water stress on NPP due to the highest projected temperatures among the suite of GCMs. The greatest gain in total carbon is projected for LPJ-CSIRO (Table I), representing the GCM with the lowest temperature increase and the second highest increase in global precipitation, in which no region shows substantial reductions in precipitation (Figure 1).

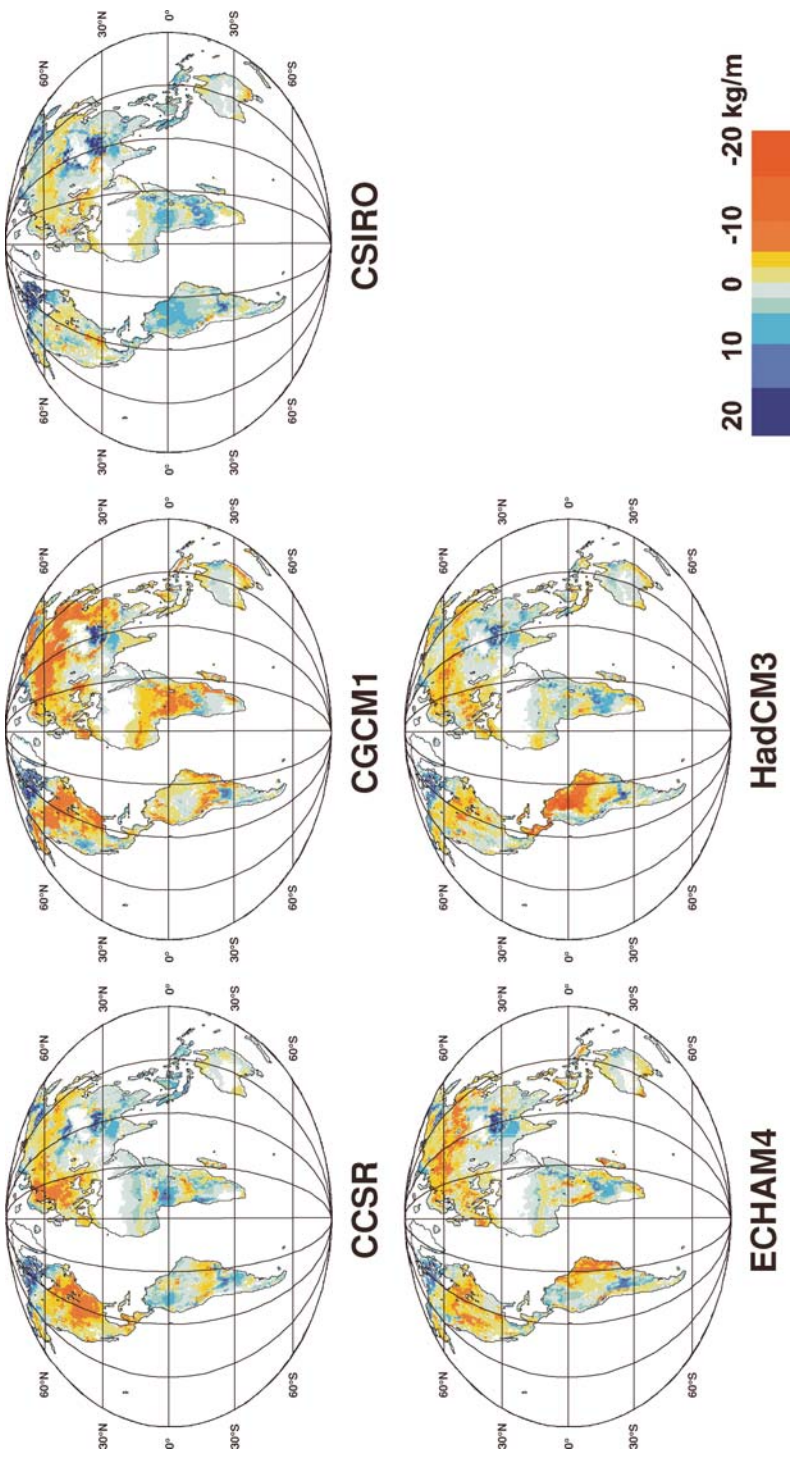

Figure 3. Changes of global terrestrial carbon storage (2071–2100 vs. 1971–2000) estimated by LPJ under 5 climate scenarios [kgC/m^2], (total carbon is the sum of all carbon pools in soil, litter and vegetation).

3.2. BROAD REGIONAL PATTERNS OF BIOSPHERIC CARBON STORAGE

Projected changes in total terrestrial carbon storage show distinct regional patterns with some areas functioning as cumulative sinks of carbon and others as cumulative sources (Figure 3). Several broad regional patterns of change in terrestrial carbon storage are found to be more or less consistent across all scenarios studied, despite the pronounced differences in the magnitude and spatial pattern of projected climate change (Figure 1). The following patterns can be identified (Figure 3):

1. *Arctic sink*. A sink occurs at high northern latitudes in Canada, and, to a limited extent, in some areas of the Siberian arctic.
2. *Boreal forest source*. All five models show carbon sources in the central areas of Eurasia and North America between about 30°N and 60°N.
3. *High-Altitude sink*. The Tibetan highlands and parts of northern India and other alpine ecosystems produce a carbon sink.
4. *Dry region sink*. Many, though not all, open grassy landscapes in Africa (especially in much of the Sahel), South America and the interior of Australia show carbon sinks in the future.
5. *Semiarid region source*. In some of the scenarios carbon source regions occur in seasonally dry regions, specifically in north-eastern South America and as a belt around the central African rainforest.
6. *Tropical source vs. sink*. Areas covered by tropical rainforest do not show a consistent response across climate models.

These regions are consistently projected to experience the most pronounced changes. We therefore examined in more detail the changes in carbon stock from 1971–2000 to 2071–2100 and the mechanisms underlying these changes. We analysed nine representative pixels in each of the respective areas. Figure 4 gives their locations and the total amount of present global carbon storage estimated by LPJ from observed climate (CRU, New et al., 2000) to enable evaluation of the future carbon changes (ensemble mean of LPJ simulations under five GCMs).

3.2.1. *Arctic Zone*

The arctic regions (Figure 4, region 1), acting as carbon sinks throughout the century, are characterized by an increase mainly in soil carbon storage. Application of bottom-up models generally indicate increased carbon storage across the domain of pan-arctic tundra, but there is substantial spatial and temporal variability that depends on the particular GCM climate scenario (McGuire et al., 2000). Increased temperature and atmospheric CO_2 concentration lead to enhanced NPP and, consequentially, more biomass. Correspondingly, increased litter fall contributes to an increase in soil carbon. In the test area studied, soil and litter carbon pools together increase on average by more than 9 (7.0 to 13.0) kgC/m^2, whereas the vegetation

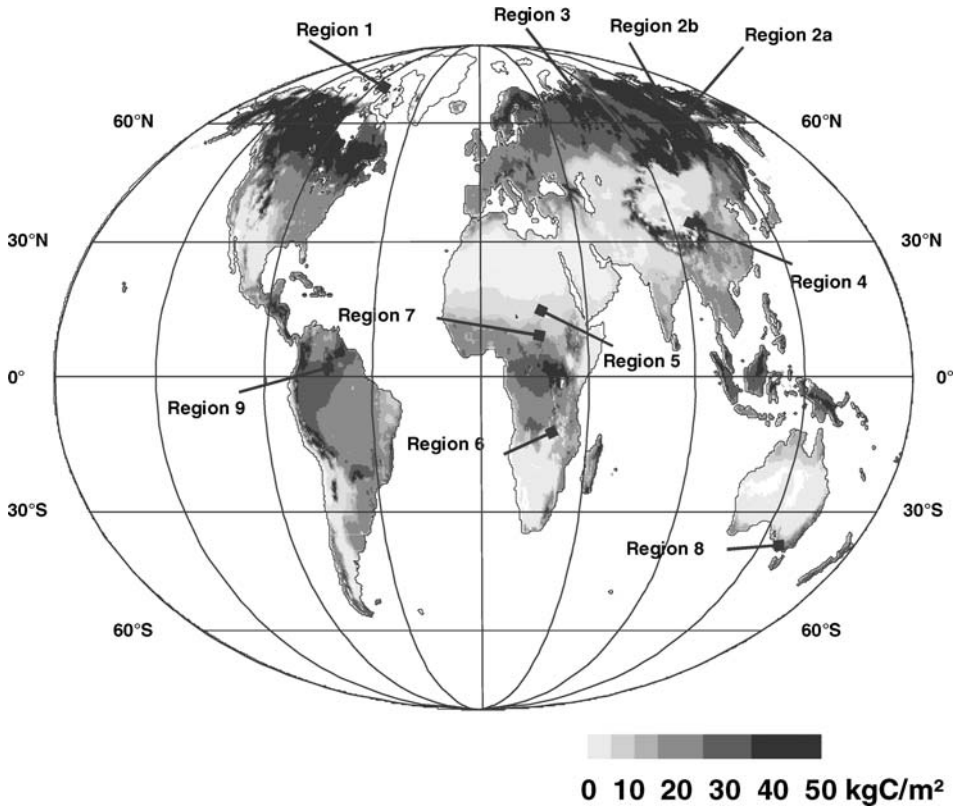

Figure 4. Global distribution of terrestrial carbon storage (kgC/m^2, average 1969–1998) as estimated by the LPJ model under observed climate (CRU, New et al., 2000). The arrows indicate the location of the regions for which changes in carbon stocks were examined in detail [see text].

pool rises by less than 1 kgC/m^2 in all scenarios (data not shown). This is due to improved conditions for growth of herbaceous vegetation while tree establishment remains difficult (Figure 5). Still higher temperatures would be necessary to enable efficient growth of trees.

3.2.2. *Boreal Zone*

According to all five scenarios the boreal tree line of the northern hemisphere is projected to migrate northwards in the course of the 21st century. This is in keeping with current trends in long-term satellite data records, which indicate a general greening trend, longer growing seasons and increased vegetation productivity for the mid to high latitudes, including the Arctic (Myneni et al., 1997; Lucht et al., 2002; Zhou et al., 2002; Nemani et al., 2003). In the test region studied (Figure 4, region 2a), previously herbaceous vegetation cover has by 2100 been replaced by boreal summergreen trees, which cover 90% of the area (Figure 6a). Increasing temperature in this zone leads to a longer growing season, enabling vegetation to

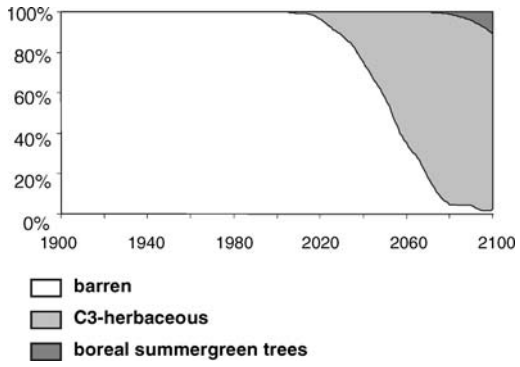

Figure 5. Partitioning (percent coverage of grid cell) of the dominant plant functional types in the arctic zone region 1 (ensemble mean of LPJ under 5 GCMs; differences between scenarios are usually <10%).

take additional advantage of increased atmospheric CO_2 concentrations. Increased NPP and plant growth result in an enhanced vegetation carbon storage of 2.2 (1.9 to 2.9) kgC/m^2 (Figure 6b and 6c, left), this increase is attributable to temperature and CO_2 change (Figure 6b and 6c, right). In this area of comparatively low temperatures and precipitation rates, soil carbon also increases by about 1.1 (-2.6 to 3.6) kgC/m^2 (Figure 6b left). Note that soil carbon decreases only in the LPJ-CGCM1 scenario, which shows the most pronounced temperature increase, which leads to an enhanced soil respiration. Beyond ca. 2070, however, all scenarios show a slight decrease in soil carbon compared to the previous years, though not strongly enough to yield values that fall below the present-day values as in CGCM1.

In contrast, a geographically similar region that, beginning in the early 21st century, equally shows the establishment of boreal summergreen trees but is characterized by higher temperatures (Figure 4, region 2b), experiences a stimulation of heterotrophic respiration. Such regions see an increased decay of their soil carbon pools where these are large, producing a net carbon source despite persistently enhanced vegetation growth (Figure 6c left). Increased precipitation (Figure 1) affects soil moisture and appears to also enhance soil respiration rates more than promote NPP. Soil carbon responds similarly to either temperature or precipitation change, whereas the simulation with constant CO_2 concentration produces a much greater source (Figure 6b and 6c, right). In the latter simulation, biomass production is lower due to absent CO_2 fertilisation, which implies lower biomass transfer to litter and soil than in the "full" simulation at the same soil respiration rate. The net effect is due to a balance between the effect of elevated temperature, which increases evapotranspiration and reduces soil moisture, dampening soil respiration, and the effect of increased CO_2 concentration on plants, which decreases stomatal conductance (Hetherington and Woodward, 2003) and, thus, transpiration, and enhances soil moisture, promoting soil respiration. In these regions with an advancing boreal tree line, the vegetation carbon increase is similar whether it occurs in areas

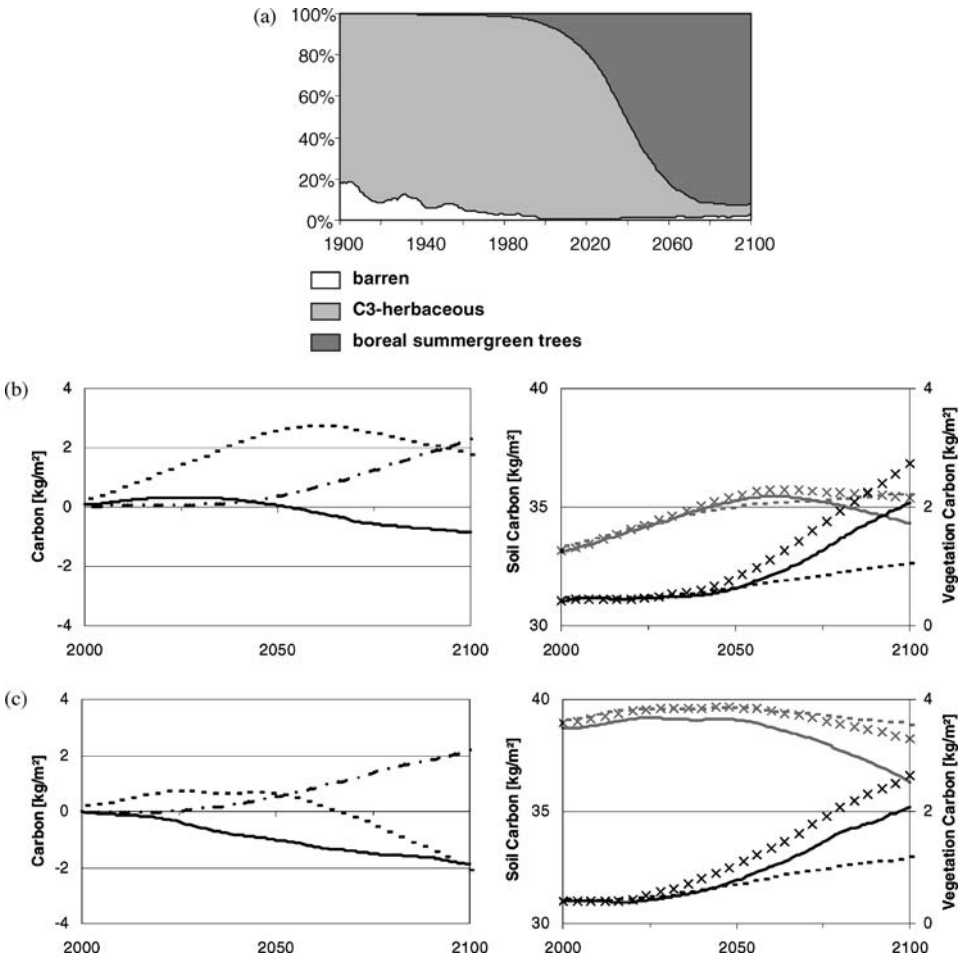

Figure 6. Time series of vegetation distribution and carbon pools in the boreal zone (region 2a & 2b), presented as the ensemble mean of LPJ simulations under the 5 GCMs. (a) Partitioning (percent coverage of grid cell) of the dominant plant functional types in both subregions (differences between scenarios are <5%); (b, c), left panel: Soil (dotted lines), vegetation (dashed-dotted) and litter carbon pools (solid) [kgC/m^2]; right panel: factorial analysis for constant temperature (dashed lines), precipitation (cross symbols) and CO_2, respectively (solid lines); vegetation (black lines) and soil carbon (grey lines). (b) region 2a of the northern carbon sink; (c) in region 2b of the northern carbon source. The differences between scenarios change little over time, i.e. the ensemble mean well represents the overall trend (mean standard deviation across scenarios: soil carbon, (b) $\pm$0.27 kgC/m^2 (c) $\pm$0.18 kgC/m^2; vegetation carbon, (b) $\pm$1.33 (c) $\pm$1.22 kgC/m^2; litter carbon, (b) $\pm$0.27 (c) $\pm$0.37 kgC/m^2).

that are overall carbon sinks (Figure 4, region 2a) or in areas that are carbon sources (Figure 4, region 2b). However, in the latter case soil carbon decreases by more than 2 (-0.1 to -4.4) kgC/m^2, in three of the five models up to 4 kgC/m^2, and the litter carbon pool declines through decomposition at about the same rate at which carbon is stored in the vegetation (compare Figure 6b and Figure 6c, left).

The primary climatic factors limiting decomposition here are low precipitation rate and low temperatures, consistent with the results of many field studies (Hobbie et al., 2002). The spatial response of decomposition is highly sensitive to changing soil moisture conditions. Accordingly, areas with large soil carbon stores and large projected increases in both temperature and precipitation are likely candidates to act as carbon source regions.

The decrease of biospheric carbon content in the northern continental belt (Figure 4, region 3) essentially reflects a reduction of the soil carbon pool. In this region the annual mean temperature is increased by about 5–6 °C by 2100 and exceeds the freezing point for two months more than today. This induces increases in heterotrophic respiration, which is additionally promoted by increased soil moisture. The upper soil layer of the model is found to be wetter in 2100, especially in spring. This is caused by increased precipitation (Figure 1). The transpiration rate is not limited by soil water supply (Schultz, 2000), and while plant growth is stimulated by higher temperature as well as by elevated atmospheric CO_2 concentration, total transpiration remains nearly unchanged. The effects of higher atmospheric CO_2concentration, i.e. decreasing transpiration as a result of increased water use efficiency (Field et al., 1995), and increased NPP ($\sim$50 g/m^2) due to higher temperature and CO_2 fertilisation effects on plants, i.e. increasing transpiration, approximately balance each other. Simulations conducted with no CO_2 increase show that the transpiration rate is about 20% higher than in the case of rising CO_2, even though in the end of the century NPP is only slightly increased due to warming. As a consequence, the vegetation carbon stabilises, and the litter and soil carbon pools decline, amplifying the carbon source. The increases in vegetation carbon are too small to counter the reduction of the soil and litter pool. The carbon source is about 5 (2.3 to 7.4) kgC/m^2 (data not shown). The composition of the vegetation in this area shows a minor shift towards boreal broadleaved summergreen trees. Due to the extent of the affected area and the magnitude of the change, the strong carbon source behaviour of the northern continental belt heavily influences the global carbon balance.

3.2.3. *High-Altitude Ecosystem*

Carbon sink behaviour in the Himalayan highlands (Figure 4, region 4) is explained by a temperature increase that facilitates the establishment of plants. In the period 1971–2000 temperature exceeded 10 °C only infrequently, and 5 °C only for 1–2 months, whereas in the period 2071–2100 5–6 month are projected to be warmer than 5 °C and temperatures are frequently above 10 °C. As a consequence, boreal trees are able to establish in addition to grassland. All carbon pools increase in size in response to the climate-driven vegetation change, especially the soil carbon pool, which is projected to increase by $\sim$13 (8 to 16) kgC/m^2 in this region within the next 100 years.

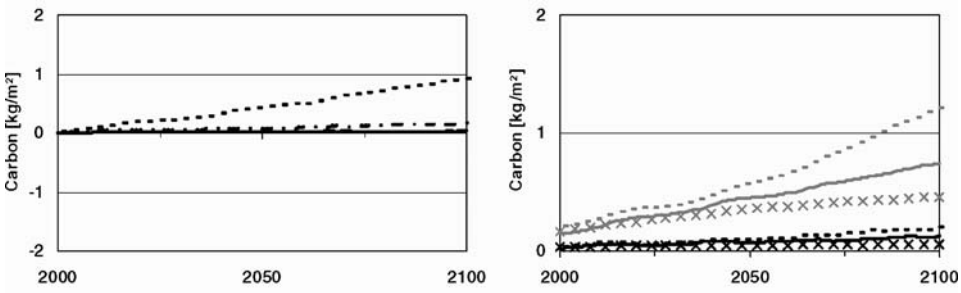

Figure 7. Time series of soil (mean standard deviation, ± 0.27 kgC/m^2), vegetation (± 0.07 kgC/m^2) and litter carbon pools (± 0.02 kgC/m^2) in region 5 of the African carbon sink (ensemble mean of LPJ simulations under the 5 GCMs). Details as in Figure 6b, c.

3.2.4. *Semi-Deserts and Savannah*

The enhanced carbon storage in dry regions of the subtropics, such as in the Sahel zone (Figure 4, region 5) or central Australia is associated with increasing water use efficiency as a consequence of rising atmospheric CO_2 concentration, which improves the conditions for establishment of plants in dry, currently barren landscapes. Factorial analyses with constant temperature (Figure 7 right) show that NPP would be higher without temperature increase. This implies that NPP suffers under drying soils in all scenarios due to higher temperature. Grasses with C4 photosynthesis are projected to take over such areas by the end of the century. Increased NPP supports subsequent storage of carbon in the soil, which results in a carbon sink where the soil is too dry to allow much decay of organic material. In the test area carbon storage increase amounts to about 1 (0.1 to 2.6) kgC/m^2 during the 21st century (Figure 7 left).

In all scenarios a carbon sink emerges in southern Africa (Figure 4, region 6). A transition in the vegetation composition from a dominance of temperate broadleaved summergreen trees and a large fraction of C3 grass to a dominance of tropical raingreen and evergreen trees takes place (Figure 8), due to rising temperatures. Here the GCMs project a temperature increase by 4 °C in three simulations, CSIRO projects about 2 °C, and CGCM1 more than 8 °C. The biospheric carbon pool is enhanced due to increases in biomass by ≈5 (2.8 to 7.4) kgC/m^2.

Total carbon stocks in northern Africa (Figure 4, region 7) are simulated to decline by about 1 (0 to 3.2) kgC/m^2 within the next 100 years, due to a reduction of soil carbon by about 1 (0.2 to 2.6) kgC/m^2 (Figure 9). This is caused by increasing soil respiration due to higher temperature at steady NPP and concurrent changes of the PFT distribution (Figure 9 left). Drought-deciduous woody vegetation establishes more strongly by the end of the century but fails to produce much biomass or to replace herbaceous vegetation and grass. Carbon stock changes remain small and affect the global carbon balance only slightly.

All scenarios show a carbon storage decrease in southern Australia (Figure 4, region 8) concerning especially the soil carbon pool (data not shown). Currently

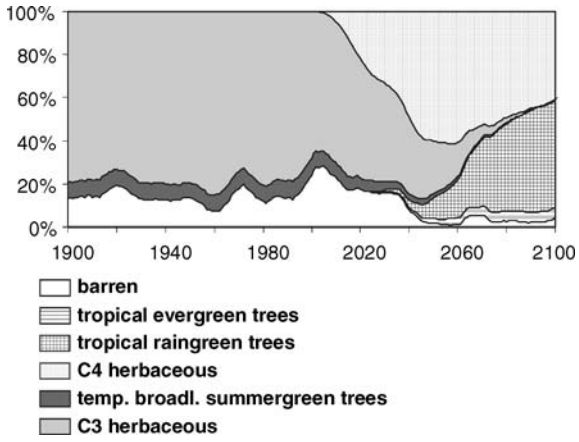

Figure 8. Partitioning (percent coverage of grid cell) of the dominant plant functional types in the southern African sink region 6 (ensemble mean of LPJ simulations under the 5 GCMs; differences between scenarios are usually <5%).

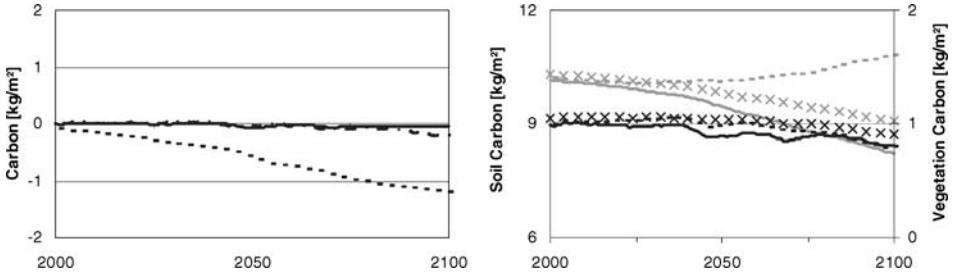

Figure 9. Time series of soil (mean standard deviation, ± 0.27 kgC/m^2), vegetation (± 0.09 kgC/m^2) and litter carbon pools (± 0.10 kgC/m^2) in region 7 of the African carbon source (ensemble mean of LPJ simulations under the 5 GCMs). Details as in Figure 6b,c.

sparsely growing broadleaved evergreen trees are replaced by grass by 2100 due to high water stress for trees. The fraction of barren land grows from 20% to up to 50%. Temperature increases more than 1 °C while annual precipitation declines by about 100 mm. These are very large changes for this arid region. Due to increasing sparsity of the vegetation cover the soil carbon pool is fed more slowly by litter fall and decreases by about 2 (0 to 3.4) kgC/m^2, as does the total carbon stock.

3.2.5. *Tropical Zone*

The tropical rainforest (Figure 4, region 9) does not show a consistent response across climate models. While some scenarios produce nearly neutral behaviour, LPJ-CSIRO produces an equatorial sink. LPJ-HadCM3 in contrast, produces a pronounced carbon source in Amazonia due to a strong decrease in precipitation leading to vegetation die-back, as dicussed by Cox et al. (2004) using the TRIFFID DGVM coupled to HadCM3. Annual precipitation in 2071–2100 is about 2000

mm in the HadCM3 scenario with significant interannual fluctuations; this equals a reduction of up to 600 mm annually compared to the current climate. This precipitation reduction is initiated by an El Niño-like pattern of sea-surface warming in the Pacific Ocean (Cox et al., 2004); stomatal closure of vegetation due to increased CO_2 concentration contributes ca. 20% to the reduction in rainfall (Betts et al. 2004). Around 29 kgC/m^2 are lost in the LPJ-HadCM3 scenario due to mortality of tropical evergreen trees, which are replaced by C4 grass. This amounts to a loss of 40 Pg biomass in the entire Amazon region. This biomass enters to the litter and soil carbon pools, and the decomposition rate and hence the release of soil and litter carbon is very fast.

4. Discussion

Simulations of biospheric carbon uptake under five different simulations of climate change driven by a common emission scenario of CO_2 increase showed moderate additional uptake of carbon by the biosphere, relatively small changes in soil carbon pools, and, after an initially continued increase, a drop in global annual biospheric carbon uptake in the second half of this century. Three out of five models switched to producing a carbon source by the year 2100 (Table I; Figure 2), that is, a positive carbon cycle feedback between climate and biosphere exists in these three scenarios. A fourth scenario shows a nearly neutral biosphere and only one scenario retains a sink. Broad spatial patterns of net source and sink behaviour over this century are relatively robust across the different climate simulations and are explained by regionally varying combinations of changes in temperature, precipitation, carbon fertilization by increased atmospheric CO_2 concentration, increased water use efficiency due to associated plant physiological responses, and vegetation composition.

Regional analysis suggests that increased future CO_2 concentrations alone will tend to increase NPP and enhance carbon storage in many areas, particularly in the North. Increasing temperature leads to longer growing seasons, increased NPP and vegetation growth and hence enhanced carbon storage. A combination of the two acts towards increasing NPP, growth and northward plant migration, i.e. carbon storage in arctic zone and northward migration of the tree line. Increased temperature also leads to increased rates of heterotrophic respiration, as shown in field experiments (Fang et al., 2005), which supports the assumption that the resistant soil carbon pools are as temperature responsive as the labile soil carbon pools. Knorr et al. (2005) show that results of soil warming experiments can be well reproduced by an Arrhenius model (Lloyd and Taylor 1994), supporting the temperature-dependence of soil repiration used in the LPJ-DGVM. In a warming climate, the resulting effect will potentially dominate the carbon balance where soil stocks are large, particularly in the boreal zone. Anaerobic conditions in soils with water-filled macropores that would restrict respiration are not explicitly considered

in the present study, as we consider only the plant-available water in our moisture calculations (Gerten et al., 2004). But, the influence of this surplus water on respiration is probably not as strong as the limiting effect of dry soils (Smith et al., 2003), which our model accounts for. Previous studies also show that there may be a transition toward aerobic respiration due to drying of soils at higher temperatures (Stieglitz et al., 2000), as this would imply an additional increase of soil respiration. Other than the boreal regions that are affected most by temperature change, tropical regions are dominated by precipitation effects; climate models show a large variability for these regions, and LPJ projects differing responses in vegetation patterns and carbon balance.

In the intercomparison of Cramer et al. (2001) among six dynamic global vegetation models forced by one climate scenario, all models projected limitations to biospheric carbon uptake, which was shown to stabilise in magnitude or decrease toward the end of this century. But the study of Cramer et al. (2001) also found considerable differences in the size of the projected changes between models. The current results show that equally large differences occur when differences in climate projection (due to differences among climate models, not differences in the assumed CO_2 scenario) are taken into consideration.

Cramer et al. (2001) used a HadCM2 climate scenario, with anomalies superimposed upon the Cramer and Leemans (unpublished data) mean climatology. Both studies were based on an IS92a emission scenario, but the biosphere simulations were conducted at the coarse spatial resolution of 3.75 by 2.5 degrees. Figure 10

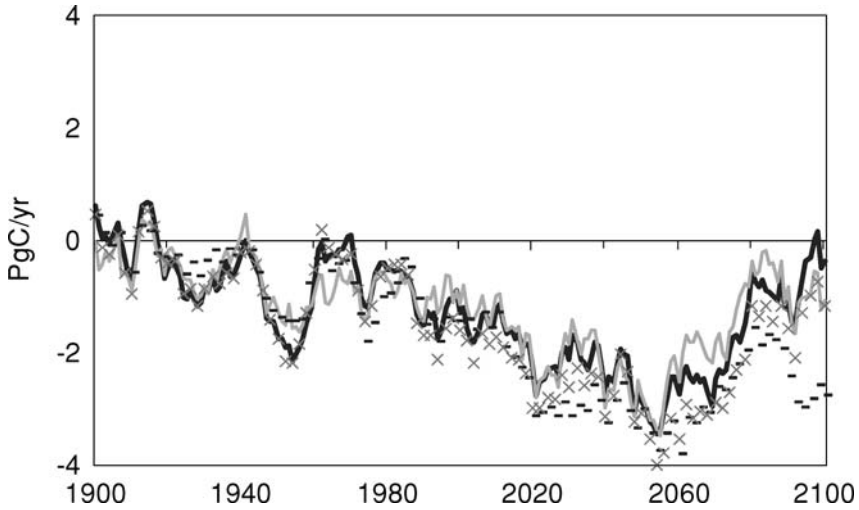

Figure 10. Comparison of global land-atmosphere flux [PgC/yr] over the period 1900–2100, as simulated by different versions of LPJ under the HadCM2 climate scenario. Dashed black line indicates the LPJ-version used by Cramer et al. (2001), solid grey line Sitch et al. (2003), cross grey symbols the Sitch et al. (2003) version with litter decomposition as in Cramer et al. (2001) and solid black line the Gerten et al. (2004) version as used in this paper.

compares the results by Cramer et al. (2001) with those from more advanced versions of the LPJ-DGVM including that used in the present paper. The difference between the current LPJ results and those from Cramer et al. (2001) is due primarily to several processes that were implemented successively in the previous model versions, and due to the effects of using a different climate scenario. First, a more rapid and more realistic litter decomposition and implementation of heat stress for boreal trees (Sitch et al., 2003), second, improved soil hydrology (Gerten et al., 2004) that resulted e.g. in stronger water stress; and third, the tendency of HadCM2 anomalies superimposed on Cramer and Leemans climatology to produce greater carbon sink strength than the climate models used here (compare Figures 2 and 10). Note that the heat stress as a bioclimatic limit for boreal trees (Sitch et al., 2003) was removed again in the present model, as its effect was compensated for by the higher water stress implemented by Gerten et al. (2004). Figure 10 demonstrates that the increase in water stress and the changed calculation of litter decomposition contributed most to the difference between the Cramer et al. (2001) study and the present study. Nevertheless, the global results are similar throughout and diverge only in the last two decades of the simulation.

Biomass and soil carbon increments documented in the present paper are smaller than those previously reported for LPJ and other models. Biomass is found to either remain almost constant (LPJ-HadCM3 and LPJ-CGCM1), or increase by at most 150 PgC (LPJ-CSIRO). Soil carbon is found to increase first and then decline, for some scenarios strongly, to yield a stock at 2100 of between 51 PgC more (LPJ-CSIRO) to 98 PgC less than in the year 2000 (LPJ-CGCM1). Cramer et al. (2001) showed biomass increases between 151 (for the LPJ-HadCM2) and 340 PgC between the years 2000 and 2100, and soil carbon increases between 28 and 220 PgC (LPJ-HadCM2 gave an increase of 111 PgC). White et al. (1999) report increases of 290 or 170 PgC, and decreases in the soil of 52 and 90 PgC, for two different climate scenarios. Already in Cramer et al. (2001) two of six models showed strongly declining carbon uptake under that climate scenario. The potential appearance of a carbon source toward the end of the century has been noted in other model experiments (Cox et al., 2000; White et al., 2000; Joos et al., 2001; Friedlingstein et al., 2001, 2003; Dufresne et al., 2002; Jones et al., 2003).

The LPJ-DGVM simulates most of the important biogeochemical processes relevant to the biospheric carbon balance. However, two major factors are not included and therefore merit discussion. These are interactions of the carbon with the nitrogen cycle and the direct impact of human activity on the carbon cycle through deforestation and agriculture.

Plant growth may be enhanced or limited by supplies of nitrogen and other nutrients. Anthropogenic N deposition can act as a fertilizer and thus reduce natural N limitations to growth. Growth enhancements due to other factors (including CO_2 and climate) are only possible if N supply is sufficient. The LPJ-DGVM uses an optimised leaf nitrogen allocation scheme, i.e. the nitrogen content of leaves is regulated in such a way as to maximise the difference between leaf carbon

uptake and respiration loss (Haxeltine and Prentice, 1996a). The model does not take account of N-supply limitations on the C allocated to leaves. Hungate et al. (2003) have suggested that the future biospheric carbon uptake reported by dynamic vegetation models exceeds the available additional nitrogen required to support this uptake. In this study, however, we find biomass increases of only 55 PgC on average (−8–151 PgC) (see Table I). These are also the maximal values for the whole of the simulation period. Soil carbon is projected to decrease or stabilise, or at most increase by 41 PgC. The largest combined increase in the simulation period is 201 PgC. Following Hungate et al. (2003) in assuming C:N ratios of 200 for trees and 15 for soils to hold (a conservative estimate because these ratios may potentially increase under elevated atmospheric carbon dioxide concentration), our simulations result in a maximal additional nitrogen demand of 4.1 PgN. Most simulations imply an additional demand of 1 PgN, or less. All of these values are well within the range of values proposed by Hungate et al. (2003).

Cultivation of land causes large releases of carbon. The biomass carried by agricultural lands is generally much less than that of the previously growing natural vegetation. Conversions from natural forest to cropland could reduce the soil carbon by up to 50% (Guo and Gifford, 2002). Land use change will most likely add a considerable carbon source term to the results reported here, though the future magnitude of this effect is difficult to estimate. It depends on many factors including population growth, agricultural productivity, and consumption patterns.

We have simulated shifts in the composition of vegetation and its spatial patterns. Such shifts occur in the wake of changes in the competitive balance between different vegetation types and in bioclimatic zones. The LPJ-DGVM encodes climatic growth limitations and processes of competition between PFTs, but some parameters governing these processes are better known than others. For example, in several previous simulations, the effects of heat stress on the reproduction of boreal vegetation led to a progressive replacement of boreal trees by grass in interior Siberia (e.g. Joos et al., 2001). The realism of this effect is uncertain and the constraint was omitted from the LPJ-DGVM runs here and by Cramer et al. (2001). Improved knowledge about vegetation dynamics on the scale of several decades is required for reducing current uncertainties in the future composition of vegetation, and thus for improved quantification of terrestrial carbon cycle projection. The LPJ-DGVM is currently being enhanced to include an interacting nitrogen cycle, agricultural land use, and an improved scheme for PFTs and their responses to climate.

5. Acknowledgements

We would like to thank Benjamin Smith and the LPJ-DGVM team for their contribution to development of LPJ, and specifically Alberte Bondeau, Kirsten Thonicke and Sönke Zaehle for valuable discussions. This work was funded by the German Ministry of Education and Research's German Climate Research Programme

(DEKLIM) under the project "Climate, Vegetation and Carbon (CVECA)". We thank the IPCC Data Distribution Centre for providing the climate scenario data.

References

Amthor, J. S.: 1995, 'Terrestrial higher-plant response to increasing atmospheric [CO_2] in relation to the global carbon cycle', *Global Change Biology* **1**, 243–274.

Betts, R. A., Cox, P. M., Collins, M., Harris, P. P., Huntingford, C., and Jones, C. D.: 2004, 'The role of ecosystem-atmosphere interactions in simulated Amazonian precipitation decrase and forest dieback under global climate warming', *Theor. Appl. Climatol.* **78**, 157–175.

Bopp, L., Le Quéré, C., Heimann, M., Manning, A. C., and Monfray, P.: 2002, 'Climate-induced oceanic oxygen fluxes: Implications for the contemporary carbon budget', *Global Biogeochemical Cycles* **16**(2), 1022, doi:10.1029/2001GB001445.

Cao, M. K. and Woodward, F. I.: 1998, 'Net primary and ecosystem production and carbon stocks of terrestrial ecosystems and their response to climatic change', *Global Change Biology* **4**, 185–198.

Cox, P. M., Betts, R. A., Jones, C. D., Spall, S. A., and Totterdell, I. J.: 2000, 'Acceleration of global warming due to carbon-cycle feedbacks in a coupled climate model', *Nature* **408**, 184–187.

Cox, P. M., Betts, R. A., Collins, M., Harris, P. P., Huntingford, C., and Jones, C. D.: 2004, 'Amazonian forest dieback under climate-carbon cycle procetions for the 21st century', *Theor. Appl. Climatol.* **78**, 137–156.

Collatz, G., Ribas-Carbo, M., and Berry, J.: 1992, 'Coupled photosynthesis-stomatal conductance model for leaves of C4 plants', *Australian Journal of Plant Physiology* **19**, 519–538.

Cramer, W., Bondeau, A., Woodward, F. I., Prentice, I. C., Betts, R. A., Brovkin, V., Cox, P. M., Fisher, V., Foley, J. A., Friend, A. D., Kucharik, C., Lomas, M. R., Ramankutty, N., Sitch, S., Smith, B., White, A., and Young-Molling, C.: 2001, 'Global response of terrestrial ecosystem structure and function to CO_2 and climate change: Results from six dynamic global vegetation models', *Global Change Biology* **7**, 357–373.

Cramer, W., Kicklighter, D. W., Bondeau, A., Moore III, B., Churkina, G., Nemry, B., Ruimy, A., Schloss, A. L., and participants of the Potsdam NPP model intercomparison: 1999, 'Comparing global models of terrestrial net primary productivity (NPP): Overview and key results', *Global Change Biology* **5**(Suppl 1), 1–15.

DeLucia, E. H., Hamilton, J. G., Naidu, S. L., Thomas, R. B., Andrews, J. A., Finzi, A., Lavine, M., Matamala, R., Mohan, J. E., Hendrey, G. R., and Schlesinger, W. H.: 1999, 'Net primary production of a forest ecosystem with experimental CO_2 enrichment', *Science* **284**, 1177–1179.

Dufresne, J. L., Friedlingstein, P., Berthelot, M., Bopp, L., Ciais, P., Fairhead, L., Treut, Le H., and Monfray, P.: 2002, 'On the magnitude of positive feedback between future climate change and the carbon cycle', *Geophysical Research Letters* **29**(10), 1405, 10.1029/2001GL013777.

Emori, S., Nozawa, T., Abe-Ouchi, A., Numaguti, A., and Kimoto, M.: 1999, 'Coupled ocean-atmosphere model experiments of future climate change with an explicit representation of sulphate aerosol scattering', *Journal of the Meteorological Society of Japan* **77**, 1299–1307.

Fang, C., Smith, P. Moncrieff, J. B., and Smith, J. U.: 2005, 'Similar response of labile and resistant soil organic matter pools to changes in temperature', *Nature* **433**, 57–59.

Farquhar, G. D., Caemmerer, S. v., and Berry, J. A.: 1980, 'A biochemical model of Photosynthetic CO_2 Assimilation in leaves of C3 Species', *Planta* **149**(2), 78–90.

Field, C., Jackson, R., and Mooney, H.: 1995, 'Stomatal responses to increased CO_2: Implications from the plant to the global scale', *Plant, Cell and Environment* **18**, 1214–1255.

Flato, G. M. and Boer, G. J.: 2001, 'Warming asymmetry in climate change simulations', *Geophysical Research Letters* **28**, 195–198.

Foley, J. A.: 1995, 'An equilibrium model of the terrestrial carbon budget', *Tellus* **47B**, 310–319.

Friedlingstein, P., Bopp, l., Ciais, p., Dufresne, J., Fairhead, L., LeTreut, H., Monfray, P., and Orr, J.: 2001, 'Positive feedback between future climate change and the carbon cycle', *Geophysical Research Letters* **28**(8), 1543–1546.

Friedlingstein, P., Dufresne, J.-L., Cox, P. M., and Rayner, P.: 2003, 'How positive is the feedback between climate change and the carbon cycle?', *Tellus* **55B**, 692–700.

Gerten, D., Schaphoff, S., Haberlandt, U., Lucht, W., and Sitch, S.: 2004, 'Terrestrial vegetation and water balance: Hydrological evaluation of a dynamic global vegetation model', *Journal of Hydrology* **286**, 249–270.

Gordon, C., Cooper, C., Senior, C. A., Banks, H. T., Gregory, J. M., Johns, T. C., Mitchell, J. F. B., and Wood, R. A.: 2000, 'The simulation of SST, sea ice extents and ocean heat transports in a version of the Hadley Centre coupled model without flux adjustments', *Climate Dynamics* **16**, 147–168.

Guo, L. B. and Gifford, R. M.: 2002, 'Soil carbon stocks and land use change: A meta analysis', *Global Change Biology* **8**, 345–360.

Haxeltine, A. and Prentice, I. C.: 1996a, 'A general model for the light-use efficiency of primary production', *Functional Ecology* **10**, 551–561.

Haxeltine, A. and Prentice, I. C.: 1996b, 'BIOME3: An equilibrium terrestrial biosphere model based on ecophysiological constraints, resource availability, and competition among plant functional types', *Global Biogeochemical Cycles* **10**, 693–709.

Hetherington, A. M. and Woodward, F. I.: 2003, 'The role of stomata in sensing and driving environmental change', *Nature* **424**, 901–908.

Hirst, A. C., Gordon, H. B., and O'Farrell, S. P.: 1996, 'Global warming in a coupled climate model including oceanic eddy-induced advection', *Geophysical Research Letters* **23**, 3361–3364.

Hobbie, S. E., Schimel, J. P., Trumbore, S. E., Randerson, J. R.: 2000, Controls over carbon storage and turnover in high-latitude soils. *Global Change Biology* **6**(Suppl 1), 196–210.

Houghton, J. T., Callander, B. A., and Varney, S. K. (eds): 1992, *The Supplementary Report to the IPCC Scientific Assessment, Climate Change 1992* Cambridge University Press, Cambridge, United Kingdom.

House, J. I., Prentice, I. C., and Le Quérè, C.: 2002, 'Maximum impacts of future reforestation or deforestation on atmospheric CO_2', *Global Change Biology* **8**, 1047–1052.

House, J. I., Prentice, I. C., Ramankutty, N., Houghton, R. A., and Heimann, M.: 2003, 'Reconciling apparent inconsistencies in estimates of terrestrial CO_2 sources and sinks', *Tellus* **55B**, 345–363.

Hungate, B. A., Dukes, J. S., Shaw, R., Luo, Y., and Field, C. B.: 2003, 'Nitrogen and Climate Change', *Nature* **302**, 1512–1513.

The Intergovernmental Panel on Climate Change (IPCC): 2001, in *Climate Change 2001: The Scientific Basis, Contribution of the Working Group I to the Third Assessment Report*, Cambridge University Press, UK.

Jones, C. D., Cox, P. M., Essery, R. L. H., Roberts, D. L., and Woodage, M. J.: 2003, 'Strong carbon cycle feedbacks in a climate model with interactive CO_2 and sulphate aerosols', *Geophysical Research Letters* **30**(9), 1479, doi:10.1029/2003GL016867.

Joos, F., Prentice, I. C., Sitch, S., Meyer, R., Hooss, G., Plattner, G.-K., Gerber, S., and Hasselmann, K.: 2001, 'Global warming feedbacks on terrestrial carbon uptake under the Intergovernmental Panel on Climate Change (IPCC) emission scenarios', *Global Biogeochemical Cycles* **15**, 891–907.

Knorr, W., Prentice, I. C., House, J. I., and Holland, E. A.: 2005, 'Long-term sensitivity of soil carbon turnover to warming', *Nature* **433**, 298–301.

Lloyd, J. and Taylor, J. A.: 1994, 'On the temperature dependence of soil respiration', *Functional ecology* **8**, 315–323

Lucht, W., Prentice, I. C., Myneni, R. B., Sitch, S., Friedlingstein, P., Cramer, W., Bousquet, P., Buermann, W., and Smith, B.: 2002, 'Climatic control of the high-latitude vegetation greening trend and Pinatubo effect', *Science* **296**, 1687–1689.

McGuire, A. D., Clein, J. S., Melillo, J. M., Kicklighter, D. W., Meier, R. A., Vorosmarty, C. J., and Serreze, M. C.: 2000, 'Modelling carbon responses of tundra ecosystems to historical and projected climate: Sensitivity of pan-Arctic carbon storage to temporal and spatial variation in climate', *Global Change Biology* **6**, 141–159.

McGuire, A. D., Sitch, S., Clein, J. S., Dargaville, R., Esser, G., Foley, J., Heimann, M., Joos, F., Kaplan, J., Kicklighter, D. W., Meier, R. A., Melillo, J. M., Moore III, B., Prentice, I. C., Ramankutty, N., Reichenau, T., Schloss, A., Tian, H., Williams, L. J., and Wittenberg, U.: 2001, 'Carbon balance of the terrestrial biosphere in the twentieth century: Analyses of CO_2, climate and land use effects with four process-based ecosystem models', *Global Biogeochemical Cycles* **15**, 183–206.

Myneni, R. B., Keeling, C. D., Tucker, C. J., Asrar, G., and Nemani, R. R.: 1997, 'Increased plant growth in the northern high latitudes from 1981–1991', *Nature* **386**, 698–702.

Nakicenovic, N. and Swart, R. (eds.): 2000, *Special Report on Emissions Scenarios*, Cambridge University Press.

Neilson, R. P.: 1995, 'A model for predicting continental-scale vegetation distribution and water balance', *Ecological Applications* **5**, 362–386.

Nemani, R. R., Keeling, C. D., Hashimoto, H., Jolly, W. M., Piper, S. C., Tucker, C. J., Myneni, R. B., and Running, S. W.: 2003, 'Climate-driven increases in global terrestrial net primary production from 1982 to 1999', *Science* **300**, 1560–1563

New, M. G., Hulme, M., and Jones, P. D.: 2000, 'Representing twentieth-century space-time climate variability, Part II, Development of 1901–1996 monthly grids of terrestrial surface climate', *Journal of Climate* **13**, 2217–2238.

Prentice, I. C., Farquhar, G. D., Fasham, M. J. R., Goulden, M. L., Heimann, M., Jaramillo, V. J., Kheshgi, H. S. , Le Quéré, C., Scholes, R. J., and Wallace, D. W. R. L.: 2001, 'The carbon cycle and atmospheric carbon dioxide', in J. T. Houghton et al. (eds.), *Climate Change 2001: The Scientific Basis*, Cambridge University Press, New York, pp. 185–237.

Prentice, I. C., Heimann, M., and Sitch, S.: 2000, 'The carbon balance of the terrestrial biosphere: Ecosystem models and atmospheric observations', *Ecological Applications* **10**, 1553–1573.

Plattner, G-K., Joos, F., and Stocker, T. F.: 2002, 'Revision of the global carbon budget due to changing air-sea oxygen fluxes', *Global Biogeochemical Cycles* **16**(4), 1096, doi:10.1029/2001GB001746.

Roeckner, E., Oberhuber, J. M., Bacher, A, Christoph, M., and Kirchner, I.: 1996, 'ENSO variability and atmospheric response in a global coupled atmosphere-ocean GCM', *Climate Dynamics* **12**, 737–754.

Ryan, M. G.: 1991, 'Sapwood Volume for three subalbine conifers: Predictive equations and ecological implications', *Canadian Journal of Forest Research* **19**, 1397–1401.

Schultz, J.: 2000, *Handbuch der Ökozonen*, Ulmer, Stuttgart.

Sitch, S., Smith, B., Prentice, I. C., Arneth, A., Bondeau, A., Cramer, W., Kaplan, J. O., Levis, S., Lucht, W., Sykes, M. T., Thonicke, K., and Venevsky, S.: 2003, 'Evaluation of ecosystem dynamics, plant geography and terrestrial carbon cycling in the LPJ dynamic global vegetation model', *Global Change Biology* **9**, 161–185.

Smith, K. A., Ball, T., Conen, F., Dobbie, K. E., Massheder, J., and Rey, A.: 2003, 'Exchange of greenhouse gases between soil and atmosphere: Interactions of soil physical factors and biological processes', *European Journal of Soil Science* **54**, 779–791.

Sprugel, D. G., Ryan, M. G., and Renee Brooks, J.: 1995, 'Respiration from the organ level to the stand', *Resource Physiology of Conifers*, Academic Press, San Diego, California, pp. 255–300.

Stieglitz, M., Giblin, A., Hobbie, J., Williams, M. and Kling, G.: 2000, 'Simulating the effects of climate change and climate variability on carbon dynamics in Arctic tundra', *Global Biogeochemical Cycles* **14**(4), 1123–1136.

Thonicke, K., Venevsky, S., Sitch, S., and Cramer, W.: 2001, 'The role of fire disturbance for global vegetation dynamics: Coupling fire into a dynamic global vegetation model', *Global Ecology & Biogeography* **10**, 661–677

Wagner, W., Scipal, K., Pathe, C., Gerten, D., Lucht, W., and Rudolf, B.: 2003, 'Evaluation of the agreement between the first global remotely sensed soil moisture data with model and precipitation data', *Journal of Geophysical Research* **108**(D19), 4611, doi:10.1029/2003JD003663.

White, A., Cannell, M. R., and Friend, A. D.: 2000: 'CO_2 stabilization, climate change and the terrestrial carbon sink', *Global Change Biology* **6**, 817–833.

Zhou, L., Tucker, C., Kaufmann, R., Slayback, D., Shabanov, N., Fung, I., and Myneni, R.: 2001, 'Variations in northern vegetation activity inferred from satellite data of vegetation index during 1981 to 1999', *Journal of Geophysical Research* **106**, 20069–20084.

Zobler, L.: 1986, 'A world soil file for global climate modelling', *NASA Technical Memorandum 87802*, NASA Goddard Institute for Space Studies, New York, U.S.A.

(Received 25 May 2004; in revised form 28 July 2005)